

Feasibility of In Vivo Imaging of Fibroblast Activation Protein in Human Arterial Walls

Meiqi Wu¹, Jing Ning², Jingle Li², Zhichao Lai³, Ximin Shi¹, Haiqun Xing¹, Marcus Hacker², Bao Liu³, Li Huo¹, and Xiang Li²

¹Department of Nuclear Medicine, State Key Laboratory of Complex Severe and Rare Diseases, Center for Rare Diseases Research, Beijing Key Laboratory of Molecular Targeted Diagnosis and Therapy in Nuclear Medicine, Peking Union Medical College Hospital, Chinese Academy of Medical Science and Peking Union Medical College, Beijing, China; ²Division of Nuclear Medicine, Department of Biomedical Imaging and Image-Guided Therapy, Medical University of Vienna, Vienna, Austria; and ³Department of Vascular Surgery, Peking Union Medical College Hospital, Chinese Academy of Medical Sciences and Peking Union Medical College, Beijing, China

Increased expression of fibroblast-activating protein (FAP) in fibrous caps may contribute to progression of atherosclerotic plaques.

Methods: Forty-one patients who underwent ⁶⁸Ga-conjugated quinoline-based FAP inhibitor (⁶⁸Ga-FAPI-04) PET/CT for noncardiovascular indications were retrospectively analyzed. Correlations were assessed between the uptake of ⁶⁸Ga-FAPI-04 in large arterial walls (SUV_{max} and target-to-background ratio, TBR) and degree of calcification and cardiovascular risk factors. **Results:** Focal arterial uptake of ⁶⁸Ga-FAPI-04 or calcification was detected in 1,177 arterial segments in all 41 patients. TBR was negatively correlated with the degree of calcification (Hounsfield units) ($r = -0.27, P < 0.01$). Mean TBR in higher-risk patients was greater than in lower-risk patients (2.2 ± 0.3 vs. $1.8 \pm 0.3, P < 0.01$). Immunohistochemical labeling of carotid plaques exhibited prominent FAP expression in a thin fibrous cap and moderate FAP expression in a thick cap. **Conclusion:** ⁶⁸Ga-FAPI-04 PET/CT might have potential for imaging fibroblastic activation in the arterial wall.

Key Words: ⁶⁸Ga-FAPI-04; fibroblast-activating protein; PET/CT; active arterial wall

J Nucl Med 2022; 63:948–951

DOI: 10.2967/jnumed.121.262863

Atherosclerosis is the primary cause of cardiovascular disease, defined by the chronic, progressive accumulation of lipids and fibrous elements in large arterial walls. The major contributors to plaque vulnerability include a large necrotic core, a thin fibrous cap, expansive remodeling, neovascularization, plaque hemorrhage, and adventitial inflammation (1). The identification of specific biomarkers of plaque vulnerability remains highly important, yet difficult (2). Destabilization of fibrous caps is mediated by collagen degeneration and the activity of extracellular proteases (1). Fibroblast-activating protein (FAP) is a type II membrane-bound serine protease (3). Preliminary ex vivo analysis detected higher FAP expression in human atherosclerotic aortic plaques than in plaque-free arterial walls; particularly, FAP expression increased in thin-capped compared with thick-capped

atheromas (4,5). Recently, the development of PET imaging using several ⁶⁸Ga-labeled FAP inhibitors (FAPIs) introduced the possibility of noninvasive, in vivo visualization of human FAP expression (6). In this study, we aimed to quantify the arterial fibroblast activation via ⁶⁸Ga-conjugated quinoline-based FAP inhibitor (⁶⁸Ga-FAPI-04) PET/CT imaging in correlation with cardiovascular risk factors.

MATERIALS AND METHODS

Patients

Forty-one patients (10 women and 31 men; mean age \pm SD, 59 ± 11 y) with suggestive hepatic lesions ($n = 27$) or IgG4-related disease ($n = 14$) underwent ⁶⁸Ga-FAPI-04 PET/CT imaging between January 2019 and January 2020. The baseline characteristics and cardiovascular risk factors were documented (Table 1). The exclusion criteria included periaortitis, vasculitis, and chemotherapy within 4 wk. The study protocol complied with the tenets of the Declaration of Helsinki and its later amendments. The study protocol was approved by the institutional review board of Peking Union Medical College Hospital, and all subjects signed an informed consent form before undergoing imaging.

Radiopharmacy and PET/CT Scans

Radiolabeling with ⁶⁸Ga-FAPI-04 was performed as previously described (7,8). All subjects underwent scans on a dedicated PET/CT scanner (Polestar m660; SinoUnion) after an uptake time of 42–70 min after intravenous injection of ⁶⁸Ga-FAPI-04 (92.5–260 MBq). After an unenhanced low-dose CT scan (120 keV, 30–50 mA), PET images were obtained from the tip of the skull to the mid thigh in 3-dimensional mode with a scan time of 2 min per bed position.

Image Analysis

We performed an active-segment analysis (target-to-background ratio [TBR] ≥ 1.6) in the 5 major arteries, including the aortic arch, ascending aorta, thoracic aorta, abdominal aorta, and iliac arteries (9). The regions of interest were manually drawn around each active segment (10-mm diameter), and SUV_{max} was determined from transaxial PET/CT images. The TBR of each active segment was derived as the segment's SUV_{max} divided by the SUV of the blood pool (average SUV_{mean} of 3 regions of interest within the vena cava). We calculated the mean TBR of all active arterial segments to assess the overall burden for each patient (9). The radioactivity in calcified arterial segments with a minimum density of 130 Hounsfield units (HU) on unenhanced CT images was also assessed (10). Two experienced nuclear medicine physicians assessed the PET/CT images. Discrepancies were reassessed by the 2 readers working in

Received Jul. 8, 2021; revision accepted Sep. 9, 2021.

For correspondence or reprints, contact Li Huo (huoli@pumch.cn).

Published online Sep. 16, 2021.

COPYRIGHT © 2022 by the Society of Nuclear Medicine and Molecular Imaging.

TABLE 1
Baseline Patient Characteristics (*n* = 41)

Characteristic	Data
Age (y)	59 ± 11
Sex ratio (female-to-male)	1:3.1
Hepatic lesion suggestive of malignancy	27 (66%)
IgG4-related disease	14 (34%)
Body mass index (kg/m ²)	23 ± 3
Risk factors	
Hypertension	12 (30%)
Diabetes mellitus	10 (24%)
Dyslipidemia	7 (17%)
Smoking	21 (51%)
History of cardiovascular event	4 (10%)

Qualitative data are number and percentage; continuous data are mean and SD.

consensus. All analyses were conducted using Hybrid 3D (Hermes Medical Solutions).

Immunohistochemistry to Assess FAP Expression in Carotid Arterial Plaques

Cryosections of tissue samples containing carotid plaques were obtained from patients who underwent endarterectomy secondary to carotid artery stenosis. Fibrous caps were identified as collagen-rich tissues visualized with elastin Masson trichrome stain separating the lumen from the necrotic core. Immunohistochemistry assessed the FAP expression with anti-FAP antibody (1:300, SP325; Abcam).

Statistics

Parametric variables are expressed as mean ± SD or as median along with first and third quartiles. Arterial segments were categorized on the basis of calcification (noncalcified [<130 HU], mildly calcified [$130\text{--}399$ HU], or severely calcified [≥ 400 HU]). Patients were divided into high-risk (prevalence of ≥ 4 cardiovascular risk factors) and low-risk (< 4 cardiovascular risk factors) groups. FAPI uptake was compared among the 3 calcification groups by 1-way ANOVAs. The variation in mean TBR for each patient in different cardiovascular risk factor groups and high-risk or low-risk groups was assessed by unpaired *t* tests. Interobserver reliability was tested in all patients with intraclass correlation coefficients using a 2-way random model applying absolute agreement. All statistical analyses were performed using SPSS Statistics (version 25, IBM Corp.). *P* values of less than 0.05 denoted statistical significance.

RESULTS

⁶⁸Ga-FAPI-04 Uptake of Active Arterial Segments and Relationship to Calcification

In total, 1,177 arterial segments of focal uptake of ⁶⁸Ga-FAPI-04 or calcification were identified in all 41 patients. The mean SUV_{max} and mean TBR for ⁶⁸Ga-FAPI-04 were 1.6 ± 0.5 and 2.0 ± 0.7 , respectively. Among all assessed arterial segments, the abdominal aorta exhibited the highest number of segments (*n* = 379), followed by the thoracic aorta (*n* = 272) and the ascending aorta (*n* = 203). Analysis of all 1,177 segments showed a significant correlation between the extent of calcification (HU) and the intensity of ⁶⁸Ga-FAPI-04 uptake (TBR) (*r* = -0.27 , *P* < 0.01;

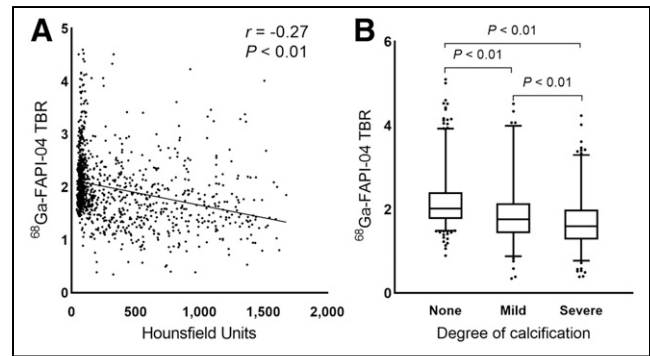


FIGURE 1. ⁶⁸Ga-FAPI-04 uptake correlates with degree of calcification in per-segment analysis (*n* = 1,177).

Fig. 1A). Noncalcified segments had significantly higher uptake (TBR, 2.2 ± 0.6 ; *n* = 603) than mildly calcified segments (TBR, 1.9 ± 0.8 ; *n* = 220) (*P* < 0.01). Severely calcified segments exhibited the lowest uptake of ⁶⁸Ga-FAPI-04 (TBR, 1.7 ± 0.6 ; *n* = 354) (*P* < 0.01) (Fig. 1B). The correlation coefficient was 0.89 (95% CI, 0.80–0.95) for interobserver agreement on TBR.

Relationship Between Arterial ⁶⁸Ga-FAPI-04 Uptake and Cardiovascular Risk Factors

The mean number of active arterial segments per patient was 29 ± 13 (range, 8–78). In the per-patient analysis, the mean TBR for ⁶⁸Ga-FAPI-04 was 1.9 ± 0.4 . The mean individual TBR was significantly higher in overweight or obese patients (body mass index ≥ 24.0 , 2.2 ± 0.4 ; *n* = 10) than in those with normal weight (1.8 ± 0.3 ; *n* = 21). There was no significant difference in ⁶⁸Ga-FAPI-04 uptake in other cardiovascular risk factor groups (Fig. 2), including male sex, older age, hypertension, diabetes mellitus, dyslipidemia, smoking habits, and past cardiovascular events. The mean TBR and the number of identified arterial segments in the high-risk patients with 4 or more cardiovascular risk factors (TBR_{mean}, 2.2 ± 0.3 ; segment number, 36 ± 17 ; *n* = 15) was significantly higher than that in the low-risk patients (TBR_{mean}, 1.8 ± 0.3 ; segment number, 24 ± 9 ; *n* = 26) (both *P* < 0.01). Figure 3 shows examples of radiotracer uptake patterns of ⁶⁸Ga-FAPI-04 in the arterial wall. All patients in the figure were over 60 y old with more than 4 cardiovascular risk factors.

FAP Expression in Human Carotid Atherosclerotic Plaques

Collagen tissue was assessed by Masson trichrome staining (Fig. 4, in blue) of human carotid arterial plaques. On the basis of the fibrous cap thickness, the specimens were characterized as thin-capped (< 65 μm) or thick-capped (≥ 65 μm) plaques. Immunohistochemical labeling with an anti-FAP antibody in sections demonstrated a prominent FAP expression in the thin fibrous cap, versus a relatively lower expression in the thick fibrous cap (Fig. 4). Specific FAPI expression localized in denatured collagen fibers (Fig. 4).

DISCUSSION

To our knowledge, this was the first noninvasive study to describe the expression of FAP in human arterial walls via ⁶⁸Ga-FAPI-04 PET/CT imaging. In this retrospective study of a noncardiovascular cohort, we observed significantly elevated uptake in noncalcified active arterial segments compared with advanced chronic lesions presenting extensive calcification, and we observed elevated ⁶⁸Ga-FAPI-04 uptake in patients with increased cardiovascular risk factors. We also found higher arterial uptake in

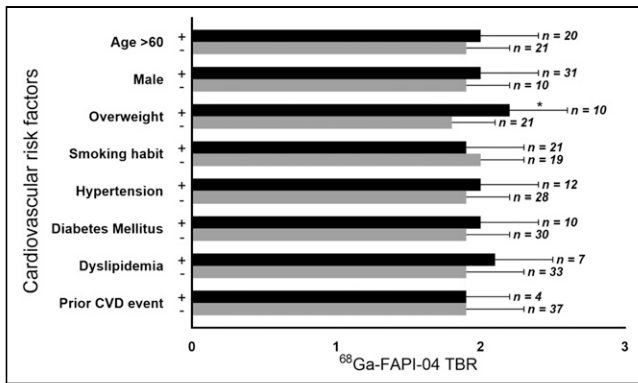


FIGURE 2. Comparison of overall arterial ^{68}Ga -FAPI-04 burden with respect to cardiovascular risk factors. CVD = cardiovascular disease. *Statistically significant difference ($P < 0.05$) in ^{68}Ga -FAPI-04 TBRs between patients who were overweight/obese or normal weight based on their body mass index.

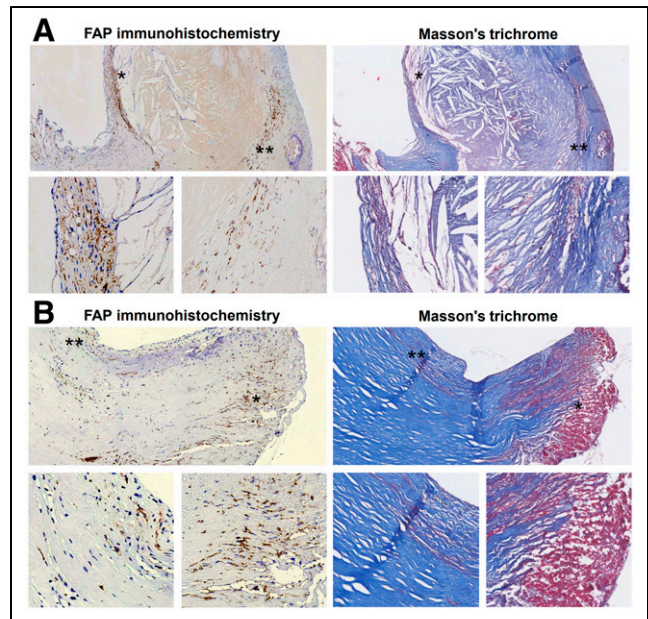


FIGURE 4. FAP expression in thin-capped (A) and thick-capped (B) human carotid atherosclerotic plaque lesions. Masson staining shows collagen-rich thin and thick fibrous caps. Plaque A had thin fibrous cap with major FAP expression (*). Fibrosis-rich region in intima also showed moderate FAP expression (**). Plaque B had thick fibrous cap with sparse FAP expression overall and FAP expression only in denatured collagen fibers (* and **).

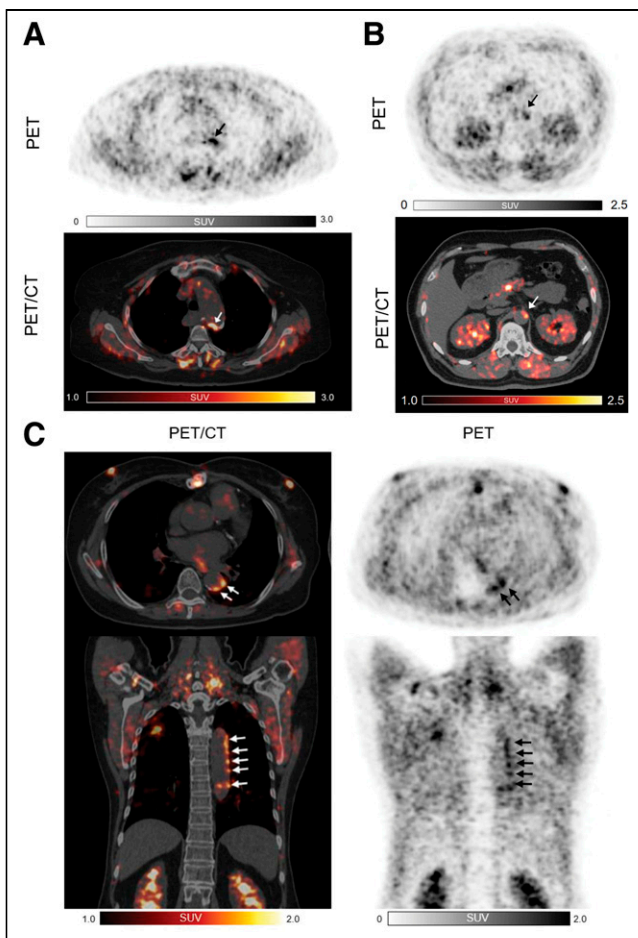


FIGURE 3. Three examples of ^{68}Ga -FAPI-04 uptake by active arterial segments. All 3 patients were over 60 y old with history of hypertension and dyslipidemia. Patients A and C also had diabetes mellitus and experienced myocardial infarction and percutaneous coronary intervention. Patient A was obese (body mass index, 30.0), and patient B had history of heavy smoking.

high-risk patients than in low-risk patients. Obesity presented a relatively more prominent impact on arterial uptake, in comparison to other cardiovascular risk factors. This observation might be related to increased image noise in obese patients.

The role of FAP in atherosclerosis is complex. Evrard et al. detected a significant number of endothelial-lineage-derived cells expressing FAP in rupture-prone, thin-capped plaques—more so than in stable plaques in atherosclerosis-prone mice and ex vivo human aortic plaques (11). Nonetheless, Monslow et al. demonstrated colocalization of FAP and vascular cell adhesion molecule 1, which marked vascular smooth muscle cells with a proliferative and matrix-producing tendency in atherosclerotic mice (12). In accordance with pioneering results from studies by Evrard and Monslow, elevated FAP expression in both thin fibrous caps and fibrosis (collagen-rich tissues in the intima) was detected in our immunohistologic findings. The role of FAP in both remodeling and stabilizing the extracellular matrix in atherosclerosis is under further investigation. Interpretation of the ^{68}Ga -FAPI-04 signal in arterial walls is challenging. We found increased FAPI uptake in noncalcified and low-level calcified lesions, compared with higher-level calcified lesions, as might indicate that aggravated fibroblast activation is irrelevant to arterial calcification burden. Nonetheless, there is a need for further evidence of arterial fibrosis quantification and calcification activation.

The retrospective and noncardiovascular nature of this study led to several inevitable limitations. The first is that the discriminatory value of FAPI uptake needs to be further validated in a cardiovascular cohort. The second is that none of the patients had concurrent histologic evidence, autoradiography, or other in vivo enhanced imaging approaches that may further facilitate identification of atherosclerotic plaques (13). The third is that scans were performed using a routine protocol that was not optimal for vessel imaging (14). The fourth is that coronary arterial lesions were not assessed because the PET scans were not cardiac-gated, with increased motion effects and partial-volume effects. Finally,

a fifth limitation is that because of the inherent limitation of unenhanced CT, noncalcified segments could be underestimated. Although we did not use the novel whole arterial segmentation method, such a method may allow a more global impression of tracer activity across vessel beds (15). Overall, our preliminary study provides a potentially feasible method to image atherosclerosis in vivo by ^{68}Ga -FAPi-04 PET/CT. Prospective studies using ^{68}Ga -FAPi-04 PET imaging in symptomatic atherosclerotic cohorts are warranted.

CONCLUSION

^{68}Ga -FAPi-04 PET/CT might have potential for imaging fibroblast activation in the arterial wall, which could provide new insights into the pathologic mechanisms. Further studies to investigate the performance of FAP imaging in symptomatic atherosclerosis cohorts are highly warranted.

DISCLOSURE

This work was sponsored in part by the National Natural Science Foundation of China (grant 82071967), CAMS Initiative for Innovative Medicine (grant CAMS-2018-I2 M-3-001), Tsinghua University-Peking Union Medical College Hospital Initiative Scientific Research Program (grant 52300300519), National Key Research and Development Program of China (grant 2016YFC0901500), and Fundamental Research Funds for the Central Universities (grant 3332020009). No other potential conflict of interest relevant to this article was reported.

KEY POINTS

QUESTION: How well does ^{68}Ga -FAPi-04 PET/CT perform for imaging of arterial walls in humans?

PERTINENT FINDINGS: In this retrospective analysis of 41 patients, we observed elevated ^{68}Ga -FAPi-04 uptake in patients with increased cardiovascular risk factors.

IMPLICATIONS FOR PATIENT CARE: ^{68}Ga -FAPi-04 PET/CT has potential as a feasible method of imaging fibroblastic activation in the arterial wall and may provide new insights into the pathologic mechanisms driving its progression.

REFERENCES

1. Finn AV, Nakano M, Narula J, Kolodgie FD, Virmani R. Concept of vulnerable/unstable plaque. *Arterioscler Thromb Vasc Biol.* 2010;30:1282–1292.
2. MacAskill MG, Newby DE, Tavares AAS. Frontiers in positron emission tomography imaging of the vulnerable atherosclerotic plaque. *Cardiovasc Res.* 2019;115:1952–1962.
3. Šimková A, Bušek P, Šedo A, Konvalinka J. Molecular recognition of fibroblast activation protein for diagnostic and therapeutic applications. *Biochim Biophys Acta Proteins Proteom.* 2020;1868:140409.
4. Brokopp CE, Schoenauer R, Richards P, et al. Fibroblast activation protein is induced by inflammation and degrades type I collagen in thin-cap fibroatheromata. *Eur Heart J.* 2011;32:2713–2722.
5. Stein S, Weber J, Nusser-Stein S, et al. Deletion of fibroblast activation protein provides atheroprotection. *Cardiovasc Res.* 2021;117:1060–1069.
6. Loktev A, Lindner T, Mier W, et al. A tumor-imaging method targeting cancer-associated fibroblasts. *J Nucl Med.* 2018;59:1423–1429.
7. Luo Y, Pan Q, Yang H, Peng L, Zhang W, Li F. Fibroblast activation protein targeted PET/CT with (^{68}Ga)-FAPi for imaging IgG4-related disease: comparison to (^{18}F)-FDG PET/CT. *J Nucl Med.* 2021;62:266–271.
8. Shi X, Xing H, Yang X, et al. Fibroblast imaging of hepatic carcinoma with (^{68}Ga)-FAPi-04 PET/CT: a pilot study in patients with suspected hepatic nodules. *Eur J Nucl Med Mol Imaging.* 2021;48:196–203.
9. Buceri J, Hyafil F, Verberne H, et al. Position paper of the Cardiovascular Committee of the European Association of Nuclear Medicine (EANM) on PET imaging of atherosclerosis. *Eur J Nucl Med Mol Imaging.* 2016;43:780–792.
10. Weiberg D, Thackeray JT, Daum G, et al. Clinical molecular imaging of chemokine receptor CXCR4 expression in atherosclerotic plaque using (^{68}Ga)-Pentixafor PET: correlation with cardiovascular risk factors and calcified plaque burden. *J Nucl Med.* 2018;59:266–272.
11. Evrard SM, Lecce L, Michelis KC, et al. Endothelial to mesenchymal transition is common in atherosclerotic lesions and is associated with plaque instability. *Nat Commun.* 2016;7:11853.
12. Monslow J, Todd L, Chojnowski JE, Govindaraju PK, Assoian RK, Pure E. Fibroblast activation protein regulates lesion burden and the fibroinflammatory response in apoe-deficient mice in a sexually dimorphic manner. *Am J Pathol.* 2020;190:1118–1136.
13. Grosse GM, Bascunana P, Schulz-Schaeffer WJ, et al. Targeting chemokine receptor CXCR4 and translocator protein for characterization of high-risk plaque in carotid stenosis ex vivo. *Stroke.* 2018;49:1988–1991.
14. Hu Y, Hu P, Hu B, Chen W, Cheng D, Shi H. Dynamic monitoring of active calcification in atherosclerosis by (^{18}F)-NaF PET imaging. *Int J Cardiovasc Imaging.* 2021;37:731–739.
15. Kwiecinski J, Tzolos E, Adamson PD, et al. Coronary (^{18}F)-Sodium Fluoride uptake predicts outcomes in patients with coronary artery disease. *J Am Coll Cardiol.* 2020;75:3061–3074.